ACS Sustainable Chemistry & Engineering

Research Article

Cite This: ACS Sustainable Chem. Eng. 2019, 7, 20032−20042

pubs.acs.org/journal/ascecg

Structural Motifs of Wheat Straw Lignin Differ in Susceptibility to Degradation by the White-Rot Fungus *Ceriporiopsis subvermispora*

Gijs van Erven,[†] Jianli Wang,[†] Peicheng Sun,[†] Pieter de Waard,[‡] Jacinta van der Putten,[§] Guus E. Frissen,[§] Richard J. A. Gosselink,[§] Grigory Zinovyev,[∥] Antje Potthast,[∥] Willem J. H. van Berkel,[†] and Mirjam A. Kabel*[,†]

[†]Laboratory of Food Chemistry, Wageningen University & Research, Bornse Weilanden 9, 6708 WG Wageningen, The Netherlands

[‡]MAGNEFY (MAGNEtic Resonance Research FacilitY), Wageningen University & Research, Stippeneng 4, 6708 WE Wageningen, The Netherlands

[§]Wageningen Food and Biobased Research, Bornse Weilanden 9, 6708 WG Wageningen, The Netherlands

[∥]Department of Chemistry, Division of Chemistry of Renewable Resources, University of Natural Resources and Life Sciences, Konrad-Lorenz-Strasse 24, A-3430 Tulln, Austria

Supporting Information

ABSTRACT: The white-rot fungus *Ceriporiopsis subvermispora* delignifies plant biomass extensively and selectively and, therefore, has great biotechnological potential. We previously demonstrated that after 7 weeks of fungal growth on wheat straw 70% w/w of lignin was removed and established the underlying degradation mechanisms via selectively extracted diagnostic substructures. In this work, we fractionated the residual (more intact) lignin and comprehensively characterized the obtained isolates to determine the susceptibility of wheat straw lignin's structural motifs to fungal degradation. Using ^{13}C IS pyrolysis gas chromatography−mass spectrometry (py-GC-MS), heteronuclear single quantum coherence (HSQC) and ^{31}P NMR spectroscopy, and size-exclusion chromatography (SEC) analyses, it was shown that *β*-*O*-4′ ethers and the more condensed phenylcoumarans and resinols were equally susceptible to fungal breakdown. Interestingly, for *β*-*O*-4′ ether substructures, marked cleavage preferences could be observed: *β*-*O*-4′-syringyl substructures were degraded more frequently than their *β*-*O*-4′-guaiacyl and *β*-*O*-4′-tricin analogues. Furthermore, diastereochemistry (*threo* > *erythro*) and *γ*-acylation (*γ*-OH > *γ*-acyl) influenced cleavage susceptibility. These results indicate that electron density of the 4′-*O*-coupled ring and local steric hindrance are important determinants of oxidative *β*-*O*-4′ ether degradation. Our findings provide novel insight into the delignification mechanisms of *C. subvermispora* and contribute to improving the valorization of lignocellulosic biomass.

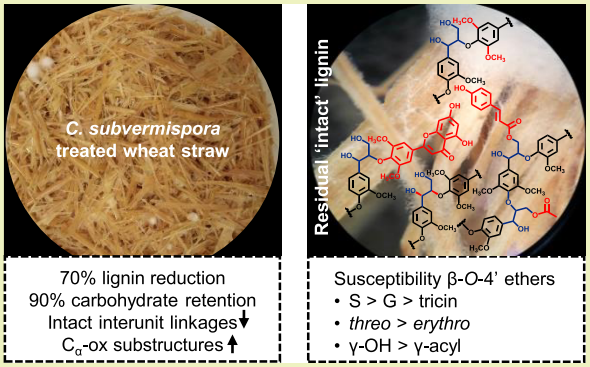

KEYWORDS: *selective delignification, biological pretreatment, lignin quantification, ligninolysis, stereoselectivity, single-electron transfer, oxidation, NMR spectroscopy*

INTRODUCTION

Most of the terrestrial fixed carbon is contained in lignocellulosic biomass, consisting mainly of cellulose, hemicellulose, and lignin. The aromatic lignin polymer plays a pivotal role in carbon recycling, as it protects the polysaccharides within lignocellulose against (enzymatic) conversion. Degradation of lignin is a crucial step in nature and is a principal goal for the industrial upgrading of lignocellulosic biomass aiming at the efficient utilization of cellulose, hemicellulose, and lignin to produce biomaterials, animal feed, biochemicals, and biofuels.[1−4] Whereas nature's strategy to overcome lignin's recalcitrance is largely based on white-rot fungi, industry currently relies on severe thermochemical pretreatments that consume extensive amounts of energy and chemicals.[5−7] Unaccompanied by such environmental impact, several white-rot fungal species degrade lignin selectively, without extensively modifying and/or degrading cellulose and hemicellulose.[8,9] Biological pretreatment as a more sustainable alternative to the physical and/or chemical pretreatment processes that are currently applied in industry is, therefore, increasingly receiving attention.[10−12]

A particularly promising white-rot fungus is *Ceriporiopsis subvermispora*. The unique effectivity and selectivity of this fungus for plant biomass delignification greatly improves ruminal and enzymatic degradability of the remaining polysaccharides.[13−17] Furthermore, this biological delignifica-

Received: September 27, 2019
Revised: October 29, 2019
Published: November 5, 2019

DOI: 10.1021/acssuschemeng.9b05780
ACS Sustainable Chem. Eng. 2019, 7, 20032−20042

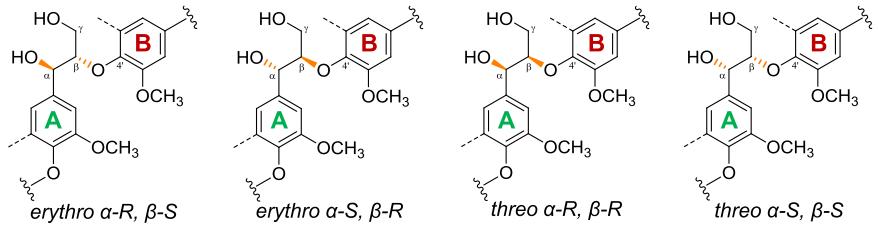

Figure 1. Diastereomers of *β-O-4′* aryl ethers. Dotted lines represent −H or $-OCH_3$ in guaiacyl and syringyl units, respectively. Wavy lines indicate main positions of further coupling within lignin.

tion does not result in inhibitory compounds for downstream processes commonly produced through chemical pretreatment.[18,19] The potential of this fungus has, therefore, been tested for a range of biotechnological applications, including biofuel production[18] and biopulping.[20,21]

An unsolved issue, impairing its industrial application thus far, is the low time efficiency of fungal delignification processes, i.e., fungal growth for extensive delignification can take up to 10 weeks.[4,22] Improving this time efficiency might be achieved through increasing our understanding of the delignification mechanisms at the molecular level. This insight contributes to the identification of the rate-limiting step(s) in the (enzymatic) oxidative process and, furthermore, might enable the selection of substrates that are more fit for purpose. Yet, the underlying delignification mechanisms are far from completely understood.

Most of our understanding of the delignification strategies employed by *C. subvermispora* is deduced from lignin model compound studies combined with genomics and proteomics research, rather than through characterization of its action on native lignin as present in lignocellulosic biomass.[23−28] As lignin model compounds usually comprise simple dimeric structures, such structures can never fairly represent degradation reactions of polymeric lignin contained in lignocellulose.

Within plant biomass, lignin occurs as a heterogeneous cross-linked macromolecule that, in grasses, is composed of *p*-hydroxyphenyl (H), guaiacyl (G), and syringyl (S) subunits. These subunits are linked through a variety of aryl ether and carbon−carbon interunit linkages, of which the *β-O-4′* aryl ether is the most abundant (∼80%). The latter *β-O-4′* aryl ethers are present as two diastereomeric pairs of enantiomers, *threo* (RR/SS) and *erythro* (RS/SR), of which the ratio is largely determined by the subunits of the interunit linkage (Figure 1).[29−32]

To add to the structural complexity of lignin, in grasses, these interunit linkages are partially esterified at the *γ*-OH position with acetate and *p*-coumarate (*p*-CA).[30,33] Additionally, a variety of ferulate and diferulate substructures are etherified to grass-type lignin, functioning as cross-linking agents between lignin and carbohydrate moieties, thereby resulting in so-called lignin-carbohydrate complexes.[34,35] Recently, the view on the complexity of grass-type lignins was even further extended, as the flavonoid tricin was found to be an integral part of this macromolecule.[30,36,37]

Although the structure of grass lignin is highly complex, *C. subvermispora* is able to effectively degrade this aromatic polymer.[13] For this purpose, the fungus relies on an oxidative enzymatic machinery that mainly depends on manganese peroxidases (MnP) and H_2O_2-generating aryl alcohol oxidases, and to a lesser extent on laccases, while lignin peroxidases (LiP) and versatile peroxidases (VP), commonly found in other white-rot fungi, are absent.[23−25] Instead, the fungal genome was found to encode two enzymes with LiP/VP-like activity, though secretome and transcriptome analyses failed to confirm their actual production during fungal growth on lignocellulose.[23−25] The collective action of the oxidative enzymes likely concerts with diffusible low-molecular-weight mediators, as lignin degradation occurs before the secondary cell wall porosity would allow enzymes to penetrate.[38−41] The exact nature and role of these mediating oxidants as well as the reactions they catalyze, however, remain unresolved.[39,40,42−44]

So far, only a few studies have been dedicated to the structural modification of actual lignocellulosic biomass during degradation by *C. subvermispora*. The studies that were conducted focused on the biodegradation of wood, of which the lignin structurally strongly differs from that of grasses. Some studies demonstrated that *β-O-4′* aryl ethers were cleaved during fungal growth, but the underlying cleavage mechanisms and relative susceptibilities of the various substructures could not be elucidated.[45−47] Yelle et al. found that spruce wood *β-O-4′* aryl ethers were majorly degraded through $C_\alpha-C_\beta$ cleavage and that this degradation proceeded diastereoselectively for the *threo*-form.[48] Contrarily, by analyzing the entire fungal-treated wheat straw samples in situ, we recently showed that grass lignin is degraded through a combination of $C_\alpha-C_\beta$ and $C_\beta-O$-aryl ether cleavages.[13] The ligninolysis pathways were unambiguously confirmed through multidimensional NMR analyses of extracts containing diagnostic substructures.[49] Despite this unprecedented in situ mechanistic insight, detailed information on the susceptibility of specific structural motifs within the lignin macromolecule, particularly those exclusively occurring in grass lignins, is yet to be obtained. Understanding of such cleavage preferences might be derived from the remaining intact substructures.

To shed further light on lignin deconstruction by *C. subvermispora*, this research aimed to comprehensively map the remaining intact lignin structures during the fungus' growth on wheat straw. Thereto, lignin in untreated and fungal-treated wheat straw after 1, 3, and 7 weeks of fungal growth was quantitatively fractionated and extensively characterized by using quantitative ^{13}C lignin internal standard (IS) pyrolysis-gas chromatography−mass spectrometry (py-GC-MS), heteronuclear single quantum coherence (HSQC) and ^{31}P NMR spectroscopy, and size-exclusion chromatography (SEC). We show that *C. subvermispora* degraded wheat straw lignin with a marked preference for *β-O-4′*-S substructures over their *β-O-4′*-G and *β-O-4′*-tricin counterparts. These *β-O-4′* ethers were, furthermore, diastereoselectively removed with a clear *threo*-preference. Acylation of the *γ*-OH moieties was shown to yield substructures more resistant against fungal attack, and as a result these substructures accumulated in the fungal-treated residue.

DOI: 10.1021/acssuschemeng.9b05780
ACS Sustainable Chem. Eng. 2019, 7, 20032−20042

MATERIALS AND METHODS

Materials. All chemicals were obtained from commercial suppliers and used without further purification. Water used in all experiments was purified via a Milli-Q water system (Millipore, Billerica, MA, USA).

Preparation of the Fungal-Treated Wheat Straw. *C. subvermispora* (CBS 347.63, *Cs*1) was used in this study.[13,15,50] Procedures for fungal strain preparation and solid-state pretreatment of the wheat straw have been previously described in detail.[13,15,50] Biological triplicates of wheat straw treated for 0, 1, 3, and 7 weeks showed minimal variation and, therefore, were thoroughly mixed in equal dry matter amounts to one replicate for further experiments and analyses.[15]

Lignin Fractionation. Lignin in untreated and fungal-treated wheat straw was fractionated according to modified procedures of Björkman and Chang et al., as presented in Figure 2.[51,52]

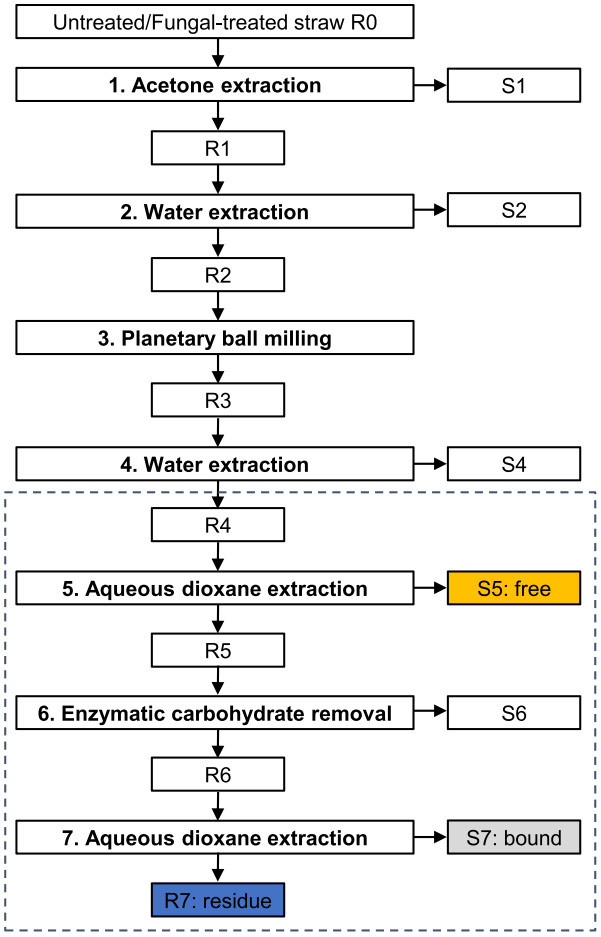

Figure 2. Fractionation scheme for untreated and *C. subvermispora*-treated wheat straw. Fractionation steps 1−4 have been described in our previous work.[49] This works describes fractionation steps 4−7, indicated with a dashed box; R: insoluble residue, S: soluble fraction.

Fractionation steps 1−4 have been described in our previous work, and therefore, will only be briefly described here.[49] Ground wheat straw (~13 g; untreated and fungal-treated) was soxhlet-extracted in triplicate with acetone and the residue was dried under reduced pressure to obtain R1. Triplicates of R1 were mixed to one replicate and extracted with water in duplicate. Residues obtained through centrifugation were freeze-dried to obtain R2. Dried duplicates were combined and planetary ball milled by using a PM100 planetary ball mill (Retsch, Haan, Germany) in batches of 3 g per 50 mL zirconium dioxide (ZrO_2) beaker containing 17 ø10 mm ZrO_2 balls, at 600 rpm with a net milling time of 4 h (excluding 10 min pauses after every 15 min of milling).

The fractionation was continued in duplicate with two portions of 12 g of milled material (R3). The remainder of the fractionation procedure was continued by using these duplicates, i.e., samples were never mixed after the respective steps. R3 was water-extracted at 5% (w/w) dry matter loading under rotary shaking (20 rpm) at 50 °C for 18 h. Insoluble material was removed by centrifugation (38 400*g*, 10 min, 20 °C) and washed twice with 130 mL of water before the material was freeze-dried to obtain R4. The dried residue (R4) was subsequently suspended in 80% (v/v) aqueous dioxane at 10% (w/w) dry matter loading and extracted twice (2 × 24 h) at room temperature with magnetic stirring (500 rpm) under a nitrogen atmosphere. The supernatants were recovered by centrifugation (30 000*g*, 5 min, 20 °C) and combined. The resulting combined supernatants and the residue were freeze-dried, washed with water to remove traces of dioxane, and freeze-dried again to obtain the dioxane-soluble fraction, S5, further referred to as "free lignin", and the dioxane-insoluble fraction, R5. R5 was incubated at 5% (w/w) dry matter and 0.025% (w/w) ViscoStar 150L protein loading in 170 mL of 50 mM sodium acetate at pH 4.8 with rotary shaking (20 rpm) at 50 °C for 16 h. Insoluble material was removed by centrifugation (30 000*g*, 5 min, 20 °C) and washed twice with 170 mL of water before the material was freeze-dried to obtain R6. R6 was dioxane-extracted in the same manner as described for R4 but without pooling the supernatants after both extraction cycles. The resulting dioxane-soluble fractions (S7-1 and S7-2) and the insoluble fraction (R7) are further referred to as "bound lignin" and "residual lignin", respectively. After every fractionation step, about 150 mg of freeze-dried material was kept apart and stored at −20 °C for further analyses.

Quantitative py-GC-MS with ^{13}C Lignin as Internal Standard (IS). Analytical pyrolysis coupled to gas chromatography with mass spectrometric detection (DSQ-II, Thermo Scientific, Waltham, MA, USA) was performed as previously described.[13,49,53] To each sample (~80 μg), 10 μL of a ^{13}C lignin internal standard (IS) solution (1 mg mL^{-1} ethanol/chloroform 50:50 v/v) was added and dried prior to analysis. All samples were prepared and analyzed in triplicate. Lignin-derived pyrolysis products were monitored in selected ion monitoring mode on the two most abundant fragments per compound (both ^{12}C and ^{13}C). Pyrograms were processed by Xcalibur 2.2 software. Lignin contents and relative abundances of lignin-derived pyrolysis products were calculated as described previously.[13,49]

Two-Dimensional (2D) HSQC NMR Spectroscopy. Around 25 mg of lignin isolate was dissolved in 0.25 mL of dimethyl sulfoxide (DMSO)-d_6 containing 0.01 M chromium(III) acetylacetonate ($Cr(acac)_3$) and pipetted into a Shigemi microcell. Two-dimensional (2D) heteronuclear single quantum coherence (HSQC) NMR spectroscopy was performed according to previously described methods.[30,54,55] The spectra were recorded at 25 °C with Bruker's standard pulse sequence "hsqcetgpsisp2.2" on a Bruker AVANCE III 600 MHz NMR spectrometer (Bruker BioSpin, Rheinstetten, Germany) equipped with a 5 mm cryoprobe located at MAGNEtic Resonance Research FacilitY (Wageningen, The Netherlands), by using the same settings as described elsewhere.[49] HSQC correlation peaks were assigned by comparison with the literature.[30,56−61] Semiquantitative analysis of the volume integrals was performed according to Del Río et al. by using TopSpin 4.0.5 software (Bruker), with previously published modifications.[13,30,49] Contours were colorized by using Adobe Illustrator software.

^{31}P NMR Spectroscopy. ^{31}P NMR spectroscopy was performed as previously described.[62] Around 30 mg of lignin isolate was mixed with 100 μL of *N*,*N*-dimethylformamide/pyridine (50:50 v/v) and 100 μL of pyridine containing 15 mg mL^{-1} cyclohexanol as internal standard and 2.5 mg mL^{-1} $Cr(acac)_3$ as a relaxation agent and stirred overnight to dissolve. Derivatization of the dissolved lignins was performed by the addition of 2-chloro-4,4,5,5-tetramethyl-1,3,2-dioxaphospholane (100 μL premixed with 400 μL of deuterated chloroform). The phosphitylated lignins were measured on a Varian 400 MHz spectrometer by using a standard phosphorus pulse sequence with 30° pulse angle (zgig30), inverse-gated proton

DOI: 10.1021/acssuschemeng.9b05780
ACS Sustainable Chem. Eng. 2019, 7, 20032−20042

decoupling, interscan delay of 5 s, and 256 scans. Signals were assigned according to Granata and Argyropoulos (1995) and integrated by using MestReNova 10 software.[63]

Size-Exclusion Chromatography (SEC). Alkaline SEC was performed as described by Constant et al. (method D).[64] Briefly, lignin isolates were dissolved in 0.5 M NaOH (eluent) in a concentration of 1 mg mL^{-1}, and the separation was performed by using two TSKgel GMPWxl columns (7.8 × 300 mm, particle size 13 μm) in series equipped with a TSKgel guard column PWxl (6.0 × 40 mm, particle size 12 μm). Absorption was monitored at 280 nm with an ultraviolet spectroscopy detector. Sodium polystyrene sulfonate (PSS) standards and phenol were used for calibration. Protobind 1000 lignin (GreenValue S.A., Switzerland) was used as reference.

Organic SEC analyses were performed as previously described.[65] Briefly, lignin isolates were dissolved in DMSO containing 0.5% (w/v) LiBr (eluent) in a concentration of 10 mg mL^{-1} and filtered through a 0.45 μm poly(tetrafluoroethylene) filter before injection. The separation was performed by using an Agilent PL gel guard column (7.5 × 50 mm) and three Agilent PolarGel M columns (7.5 × 300 mm, particle size 5 μm) in series.[66] Protonated PSS standards were utilized for calibration of the columns and refractive index and UV (280 nm) for detection. To obtain a more accurate molar mass, correction factors from multi-angle light scattering (MALS) were applied as previously described.[65]

Carbohydrate Content and Composition. Carbohydrate content and composition were determined in duplicate as constituent monosaccharides after acid hydrolysis by a modified method reported by Englyst and Cummings (see the Supporting Information for details).[67]

RESULTS AND DISCUSSION

Fungal Delignification of Wheat Straw. We previously described that *C. subvermispora* is able to effectively and selectively delignify wheat straw during 7 weeks of growth [70% (w/w) lignin removal, 90% (w/w) carbohydrate retention] and showed through in situ analyses that the residual lignin was extensively altered in structure (see Figure S1 and Table S1 for new data of additional time points).[13] Although the use of these in situ analyses ensured that the entire sample was analyzed, the whole cell wall NMR analyses suffered from overlapping carbohydrate signals in the interunit linkage region. To allow a more comprehensive and in-depth structural characterization of residual lignin in fungal-treated straw, lignin was fractionated according to the scheme presented in Figure 2. In a recent work, we showed that diagnostic truncated structures were selectively extracted in fractionation steps 1−4, which enabled us to elucidate multiple in situ delignification pathways.[49] In the current work, we focused on the intact structural motifs that remained after fungal action to determine their relative susceptibilities to degradation. To that end, we analyzed the lignin remaining in the ball-milled water-insoluble residue (R4). Similar relative amounts of lignin (~70% w/w) were recovered in this fraction for all time points, allowing a fair comparison.[49]

Fractionation of Untreated and Fungal-Treated Wheat Straw Lignin. Lignin in the ball-milled water-insoluble residue (R4) was quantitatively fractionated into "free", "bound", and unextractable (residue) lignin, achieving >90% recovery in these three fractions at all time points (Figure 3).

A slight but significant ($P < 0.05$) increase in unextractable lignin (res) was found after 3 and 7 weeks of fungal treatment, although at all time points, the combined extractable fractions (free + bound) summed up to ~80% of R4. Hence, the lignin fractions obtained were considered highly representative of the total lignin as present in the (residual) starting material. Yields

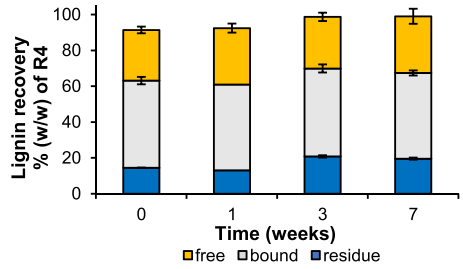

Figure 3. Recovery of lignin isolates. Recoveries were determined by using ^{13}C-IS py-GC-MS. Average and standard deviation of analytical duplicates of fractionation duplicates. One fractionation replicate was obtained for bound and residue fractions of the week 1 sample. See Figure 2 and the experimental section for lignin fractionation details; free directly dioxane-extractable, bound dioxane-extractable after enzymatic carbohydrate degradation, and "residue" dioxane-unextractable.

for free and bound lignin were comparable to what has previously been reported for similar lignin isolations from untreated wheat straw.[30,68,69] To obtain a representative sample without unintentional degradation and further fractionation, the lignin isolates were not chemically purified.[51,52] The purities of the crude isolates were comparable to what has previously been achieved with isolation schemes in which chemical workup was omitted (Table S2).[51,52,69] In all isolates, carbohydrates were the major impurity and ranged from 14 to 26% (w/w). Other impurities most likely comprised fungal metabolites, especially in free lignin fractions.

Structural Features of Lignin Isolates. Besides yield, also structure-wise the obtained isolates were highly representative of the lignin present in R4 (Tables S3 and S4). Note that in regular py-GC-MS analyses, i.e., in the absence of methylating agents such as tetramethylammonium hydroxide, the origin of vinyl products cannot be deduced.[70,71] Upon pyrolysis, these products arise from lignin's interunit linkages as well as from decarboxylation reactions of hydroxycinnamic acids, in grasses mainly ferulate and *p*-coumarate, yielding 4-vinylguaiacol and 4-vinylphenol, respectively.[30,71] Compared to R4, the isolates showed very similar relative distributions of pyrolysis products, except for a decrease in such vinyl products. As ferulates and, to a lesser extent, *p*-coumarates were attached to polysaccharides, they were more retained in the dioxane-insoluble residue R7 (Table S5). Furthermore, these substructures were partially solubilized, and hence removed, during enzymatic carbohydrate removal (data not shown). The fact that the fractions R4 and R7 showed close to identical relative distributions of pyrolysis products further highlights that representative isolates were obtained. Additionally, this implied that R7, with low lignin contents (6−13% w/w), could be fairly excluded from detailed structural analyses without affecting the overall insights obtained.

SEC analyses of the isolates confirmed that polymeric lignins were obtained, also after fungal growth (Figure S2). Alkaline SEC of free lignin isolated from untreated straw showed a weight-average (M_w) molecular mass of 3535 g mol^{-1} and a number-average (M_n) molecular mass of 1650 g mol^{-1}, resulting in a relatively narrow dispersity (M_w/M_n, $Đ$) of 2.1, which is in agreement with previous lignin isolations from wheat straw.[30,69] Bound lignin of untreated straw showed considerably larger molar masses, with 5280[1] and 2155 g

DOI: 10.1021/acssuschemeng.9b05780
ACS Sustainable Chem. Eng. 2019, 7, 20032−20042

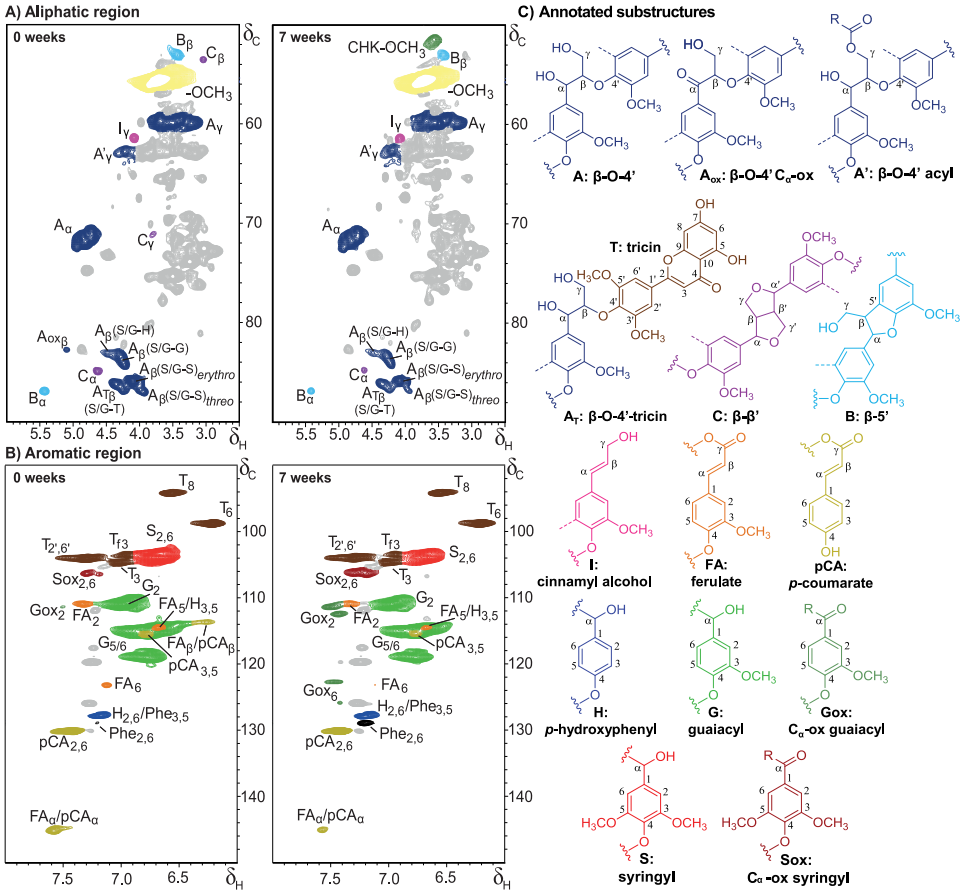

Figure 4. Aliphatic (A) and aromatic (B) regions of $^{1}H-^{13}C$ HSQC NMR spectra of free lignin isolates from untreated (left) and 7 week *C. subvermispora*-treated (right) wheat straw and annotated substructures (C). Dotted lines represent −H or $-OCH_3$. Wavy lines indicate main positions for further coupling. Chemical shift assignments are reported in Table S6. Unassigned signals in gray; amino acid residues (Phe, phenylalanine) in black. The aromatic regions of free lignin isolates presented correlation peaks of impurities and/or isolation artifacts, at similar intensities in untreated and treated samples. These unassigned peaks could be removed by classic Björkman chemical purification, but this purification also led to further fractionation of the lignin due to the fact that a major part of the lignin remained insoluble in 2:1 dichloroethane/ethanol (data not shown).[51] As the unassigned peaks were well resolved and, therefore, expected not to interfere with our analysis, purification of the samples was not performed.

mol^{-1}, for M_w and M_n, respectively, again displaying a relatively narrow dispersity ($Đ \sim 2.5$). Considerably higher molecular weights of the untreated isolates were obtained by organic SEC analyses, in particular after employing correction factors for the conventional calibrant calculated on the basis of SEC-MALS analyses ($M_{w,free}$ 17 630 g mol^{-1}, $M_{w,bound}$ 29 920 g mol^{-1}).[65] Although higher dispersities were obtained by organic SEC analyses ($Đ \sim 3.6$), they were still lower than that reported for a comparable lignin isolate ($Đ \sim 5$) that was analyzed in the same manner.[65] All lignin isolates of fungal-treated samples exhibited comparable dispersities and displayed only a slightly decreasing trend in M_w over fungal growth time (Figure S2).

A closer look at the py-GC-MS analyses indicated a slight decrease of S-units in the lignin isolates during fungal growth ($H/G/S_{t=0}$ 9:63:29 vs $H/G/S_{t=7}$ 9:67:24 in free isolates), besides an increase of C_α-oxidized and unsubstituted pyrolysis products at the expense of products with an intact three-carbon side chain (PhCγ) (Table S4). As discussed previously for the whole samples, these observations indicated the presence of degraded interunit linkages.[13] The presence of truncated structures was further demonstrated by substantial levels of benzyl diketones, pyrolysis markers for dihydroxypropiovanillone/syringone substructures.[49] Assignment of the specific linkages that were degraded during fungal growth was further substantiated by HSQC NMR analyses. Representative HSQC NMR spectra of free isolates of untreated and 7 weeks *C. subvermispora*-treated wheat straw are presented in Figure 4, for which assignments were based on the literature.[30,56−61] As mentioned above, particularly the aliphatic region (δ_C/δ_H 50−90/2.5−6.0) benefitted from lignin isolation and showed clear lignin-derived signals (Figure 4A). Several substructures of the *β-O-4′* interunit linkages could be resolved. Besides the often-reported distinction between acylated (A'_γ) and non-acylated, γ-OH substructures (A_γ), we also distinguished *β-O-4′* linkages to tricin (A_T) from those linking lignin subunits (A), by their respective C_β/H_β correlations.[61] Note that other *β-O-4′* aryl ether substructures bound to S-units with electron-withdrawing substituents might overlap with the $A_{T\beta}$ correlation peak.[56] However, most, if not all, of the signal is constituted by S/G-*β-O-4′*-T units, as deduced from semiquantitative analyses of the volume integrals of the $A_{T\beta}$ and $T_{2',6'}$ peaks.

S/G-*β-O-4′*-S and S/G-*β-O-4′*-G linkages, where the 4′-linked subunit represents ring B in Figure 1, were, furthermore, clearly resolved. In addition, the C_β/H_β correlations of the *erythro*- and *threo*-diastereomers of S/G-*β-O-4′* linkages to S-

DOI: 10.1021/acssuschemeng.9b05780
ACS Sustainable Chem. Eng. 2019, 7, 20032−20042

Table 1. Semiquantitative HSQC NMR Structural Characterization of Lignin Isolates of Residual Wheat Straw during Growth of *C. subvermispora*

	free (weeks)				bound (weeks)			
	0	1	3	7	0	1	3	7
lignin subunits (%)[a]								
H	3	3	3	2	3	3	3	3
G	59	60	55	55	57	56	57	62
G_{ox}	0	1	6	11	0	1	2	4
S	35	33	28	23	40	38	33	28
S_{ox}	3	3	7	9	1	2	5	4
S/G	0.6	0.6	0.6	0.5	0.7	0.7	0.6	0.5
hydroxycinnamates (%)[b]								
p-coumarate	10	9	11	13	5	5	4	4
ferulate	5	5	6	4	5	6	6	6
flavonolignin (%)[b]								
tricin	13	12	14	15	6	6	7	9

[a]Relative distribution of lignin subunits (H + G + G_{ox} + S + S_{ox} =100). [b]Relative volume integral of substructure versus volume integral of total lignin subunits.

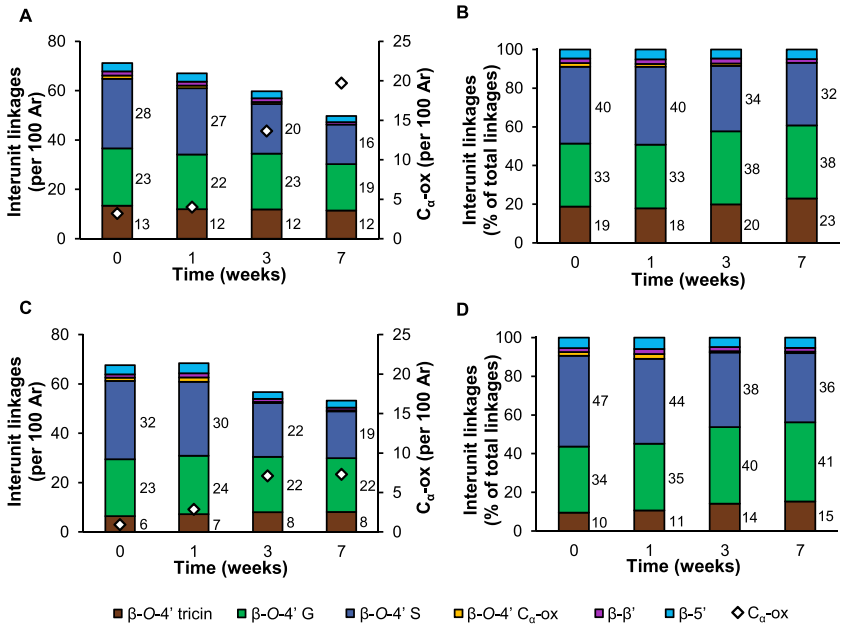

Figure 5. Semiquantitative HSQC NMR analysis of intact interunit linkages in lignin isolates of residual wheat straw during growth of *C. subvermispora*. (A, B) Free lignin isolates; (C, D) bound lignin isolates. Ar: aromatic rings.

units presented well-isolated signals. The diastereomers linked to G-units could, as expected, not be discriminated.[56]

Phenylcoumaran (*β*-5′) and resinol (*β*-*β*′) substructures were readily observed as well, whereas C_α-oxidized (*α*-keto) *β*-*O*-4′ substructures required higher zoom levels in the isolates of 7 weeks treated straw. Dibenzodioxocins (5-5′/4-*O*-*β*′) and spirodienones (*β*-1′/*α*-*O*-*α*′) were only observed at zoom levels where other correlation peaks started to overlap, and were, therefore, excluded. In the aromatic region (Figure 4B), typical wheat straw lignin signals were observed ($S_{2,6}$, G_2, $H_{2,6}$, and several tricin (T), *p*-CA, and FA related signals).[30,72] Several signals related to C_α-oxidized aromatic units became more apparent in fungal-treated samples.[13] A summary of the semiquantitative analyses of the volume integrals (Figure 4) is presented in Table 1 for main aromatic units and in Figure 5 for interunit linkages.

Besides the use of an adiabatic pulse sequence, semiquantitative analyses benefited from the relatively similar polydispersities of the lignin isolates, given the fact that quantification accuracy is largely dependent on the molecular weight distribution of the components in the sample.[73,74] In an attempt to further improve the accuracy, the HSQC spectra were recorded in the presence of $Cr(acac)_3$, a relaxation agent that is commonly employed in one-dimensional NMR analyses, such as ^{13}C and ^{31}P NMR, but is, to the best of our knowledge, not considered for application with HSQC NMR analysis.[64,75] We found that the presence of $Cr(acac)_3$ reduced the overestimation of pendant/end-group units attached to the lignin polymer (*p*-CA, FA, and T; Table 1 and Table S7).[30,37,55] In addition, we noticed a suppression of resinol substructures in the presence of $Cr(acac)_3$, which could analogously indicate that they occur as pendant units. The other structural characteristics, including those targeted by fungal action, were not extensively affected (Table S7). Therefore, the addition of $Cr(acac)_3$ might help in providing

DOI: 10.1021/acssuschemeng.9b05780
ACS Sustainable Chem. Eng. 2019, 7, 20032−20042

more accurate insight into the actual distribution of lignin's structural features by HSQC NMR.

The overall lignin subunit composition of both the free and bound isolates (Table 1) matched very well with what we previously observed by using whole cell wall NMR on unfractionated samples.[13] Again, a preference for the removal of S-units could be recognized ($H/G/S_{t=0}$ 3:59:38 vs $H/G/S_{t=7}$ 2:66:32 in free isolates). C_α-oxidized substructures steadily accumulated upon fungal action and were predominantly found in free lignin isolates, where they comprised up to 20% of all lignin subunits after 7 weeks of fungal growth (Table 1). Tricin and *p*-CA substructures accumulated during fungal growth as well, whereas ferulates appeared rather stable. These findings will be further discussed in the next section.

Susceptibility of Lignin's Structural Motifs to Fungal Degradation. Fungal action resulted in a clear reduction of intact interunit linkages in both free (from 70 to 50 per 100 subunits) and bound (from 68 to 53 per 100 subunits) lignin fractions during 7 weeks of treatment (Figure 5). With the decrease in intact interunit linkages, C_α-oxidized substructures increased, without a concomitant increase in C_α-oxidized *β*-*O*-4′ interunit linkages. Therefore, we imply that the signal of C_α-oxidized substructures originated from cleavage products that remained attached to the polymer. The latter is inferred from the fact that no low-molecular-weight material was present in the lignin isolates (Figure S2). Although the intact interunit linkages clearly decreased upon fungal action, the molecular weight of isolated lignins remained rather constant, which might point to the occurrence of repolymerization reactions (Figures 5 and S2). Such repolymerization reactions, presumably driven by radical chemistry, might also have involved some (initially released) C_α-oxidized substructures.

In accordance with these findings, ^{31}P NMR spectra showed an increase in carboxylic acid residues during fungal growth as well as an increase in phenolic hydroxyl groups (Table S8). Neither py-GC-MS nor HSQC NMR analyses suggested the presence of demethylated subunits and, therefore, we inferred that the increase in phenolic hydroxyl groups was solely due to the cleavage of phenolic and non-phenolic interunit linkages.[76] We concluded that the rate of formation of free phenolic hydroxyl groups exceeded the rate of removal and, consequently, that free phenolic subunits were not preferentially targeted over their non-phenolic analogues, even though the former subunits are generally regarded to be more susceptible to (enzymatic) oxidative degradation.[77,78]

Our results showed that the relative proportion of *β*-*O*-4′ aryl ethers (total) to *β*-5′ and *β*-*β*′ substructures was relatively constant during fungal growth (Figure 5B,D). The more condensed C−C linked structures, thus, appeared to have a similar susceptibility to fungal degradation/removal as compared to *β*-*O*-4′ aryl ethers.

Conflicting results have previously been reported on the susceptibility of condensed linkages to degradation by *C. subvermispora*. Using model compounds, Daina et al. showed that a phenolic *β*-5′ phenylcoumaran structure was efficiently degraded, whereas its non-phenolic counterpart was almost completely resistant.[28] In actual biomass, a preferential removal of *β*-*O*-4′ aryl ethers as compared to condensed linkages was found in loblolly pine, whereas *β*-5′ phenylcoumarans and *β*-*β*′ resinols seemed to be more effectively removed from white spruce.[45,48] It is important to note that the latter observations were derived from isolates that were obtained in low yields (<5%), due to which it cannot be excluded that certain lignin populations were underrepresented. Not only the type of interunit linkage but also the substructures constituting the linkage, e.g., the A- and B-ring subunits, might influence the susceptibility to degradation.

Indeed, in wheat straw, the different substructures of the *β*-*O*-4′ aryl ethers showed pronounced differences in cleavage susceptibility. *β*-*O*-4′ aryl ethers linked to S-units (ring B, Figure 1) were found to be considerably more degraded by *C. subvermispora* than their counterparts linked to G-units (S/G-*β*-*O*-4′-S > S/G-*β*-*O*-4′-G). After 7 weeks of fungal growth, *β*-*O*-4′-S units were depleted by approximately 40% in both free and bound fractions, whereas *β*-*O*-4′-G units were depleted by 19 and 6% in these fractions, respectively (Figure 5).

S-units have previously been described to be more susceptible to fungal action than G-units, and this was suggested to be caused by a lower redox potential and the absence of condensed carbon−carbon linked structures as an effect of the additional methoxyl group in S-units.[79] We showed that the preferential degradation of S-units was also maintained within interunit linkages of the same type and, thus, that the preference was not only due to the degree of condensation. More specifically, our results indicated that the cleavage of *β*-*O*-4′ aryl ether linkages was influenced by the degree of methoxylation of the 4′-*O*-coupled subunit. Due to the fact that *β*-*O*-4′ ethers differing in the degree of methoxylation of subunit A are not resolved in the (regular) HSQC NMR spectra of non-acetylated samples, it cannot be further specified whether the degree of methoxylation also affected the cleavage of linkages attached to the 1′-position of that subunit.

In addition, when the 4′-*O*-coupled ring was part of a tricin molecule that was incorporated into the lignin polymer, the susceptibility to degradation was reduced even further. In free and bound lignin fractions, *β*-*O*-4′-tricin aryl ethers relatively accumulated, and this effect was the largest in the latter fractions (Figure 5D, *β*-*O*-4′-$\text{tricin}_{t=0}$ 10% vs *β*-*O*-4′-$\text{tricin}_{t=7}$ 15%).

Besides the structure of the B-ring, diastereochemistry was shown to impact the susceptibility to degradation of *β*-*O*-4′ aryl ethers (Table 2). By comparing the *threo*- and *erythro*-diastereomers of *β*-*O*-4′-S units during fungal growth, we found that these linkages were depleted with a marked *threo*-preference. This gave rise to an increase in the *erythro*/*threo* ratio in the free lignin isolates from 2.2 to 4 after 7 weeks of fungal growth (Table 2). Bound lignin isolates also displayed the diastereoselective removal of *β*-*O*-4′ units, although to a much lesser extent.

Table 2. Degree of *γ*-Acylation and Diastereomer Ratio of *β*-*O*-4′ Aryl Ethers in Lignin Isolates of Residual Wheat Straw during Growth of *C. subvermispora*. Determined Using Semiquantitative HSQC NMR Spectroscopy

	free (weeks)				bound (weeks)			
	0	1	3	7	0	1	3	7
γ-acylation (%)	10	13	14	16	23	24	23	25
erythro/*threo*[a]	2.2	2.6	2.8	4.0	2.6	2.5	2.9	2.9

[a]Ratio of $A_\beta(S/G\text{-}S)_{erythro}$ and $A_\beta(S/G\text{-}S)_{threo}$; diastereomers for *β*-*O*-4′ aryl ethers coupled to G-units were not resolved.

The formation of *threo*- or *erythro*-diastereomers during lignin biosynthesis is determined by both of the subunits (rings A and B) to which the linkage is bound. While S-units

DOI: 10.1021/acssuschemeng.9b05780
ACS Sustainable Chem. Eng. 2019, 7, 20032−20042

preferentially form *erythro*-diastereomers, also reflected in the *erythro*/*threo* ratio of untreated straw lignin isolates, G-units link without a diastereomeric preference.[31] Based on selectivity for *threo*-diastereomers alone, a preferential removal of *β*-*O*-4′ aryl ethers linked to G-units might, thus, be expected. The fact that a total preference for the removal of *β*-*O*-4′-S units still prevailed could indicate that the degree of methoxylation of the B-ring is a stronger determinant for susceptibility than stereoisomerism. Diastereoselectivity for the degradation of the *threo*-isomers by *C. subvermispora* has been demonstrated before on spruce wood, consisting entirely of G-units.[48]

Even though tricin takes part in the same combinatorial radical coupling processes that occur between monolignols, with its dimethoxylated ring acting like a regular S-unit, it is uncertain whether tricin's B-ring steers the formation of diastereomers in a similar fashion.[31,36] Tricin is considered to be incorporated in the macromolecule majorly via binding to G-units (G-*β*-*O*-4′-tricin), so it can be postulated that the tricin-bound *β*-*O*-4′ aryl ethers should be present without a clear diastereomeric preference.[31,37] The latter was also observed in tricin oligolignols extracted from maize and biomimetic coupling reactions between coniferyl alcohol and tricin.[36,80] Thus, the fact that tricin-containing substructures appeared to be more resistant against fungal degradation was unlikely to be an effect of stereochemistry alone. A slight shift in the ratio of the correlation peaks belonging to *β*-*O*-4′ tricin substructures was observed, which did suggest a different susceptibility of the different isoforms of tricin-containing substructures. C_β-H_β peaks of *β*-*O*-4′ tricin substructures were, however, not sufficiently resolved to further speculate which substructure was degraded more extensively.[61]

In addition to tricin incorporation, the incorporation of acyl groups at the *γ*-OH position of *β*-*O*-4′ aryl ethers influenced the susceptibility to degradation. In free lignin isolates, *γ*-acylated substructures accumulated from 10 to 16%. Acylation levels in untreated straw were comparable to what has previously been reported for similar wheat straw lignin isolates.[30,72] From the relatively low levels of *p*-coumarate in bound isolates, it was deduced that *γ*-acyl groups were largely composed of acetates. Due to the fact that the levels of *γ*-acylation remained rather constant in bound isolates, the presence of *γ*-acetates seemed to have influenced the degradability to a lesser extent than *p*-coumarates, which might be explained by the bulkiness of the esterifying group. The fact that tricin incorporation and *γ*-acylation yielded substructures more resistant against degradation might (partially) explain why we previously observed that *C. subvermispora* more efficiently degraded wheat straw lignin as plant maturity increased.[16] In younger plant tissues, the relative levels of tricin and *γ*-acylated substructures were higher.[33,36,59]

Mechanistic Insight into the Delignification Mechanisms of *C. subvermispora*. The clear difference in susceptibility of various *β*-*O*-4′ aryl ether substructures provided new insight into the underlying delignification mechanisms.

The apparent B-ring dependence indicated that the effects of subunit oxidation were, at least for a substantial part, exerted on the linkages attached to the 4′ position. Not only is this in line with the previously reported high abundance of *β*-*O*-l4′ aryl ether cleavage reactions, it also supports the very argument that ligninolysis is initiated by single-electron transfer (SET) oxidation.[49] In accordance with SET oxidation, the decreasing susceptibility in the order *β*-*O*-4′-S > *β*-*O*-4′-G > *β*-*O*-4′-tricin suggests that electron density of the 4′-*O*-coupled ring is an important driving force for degradability. Whereas methoxyl groups increase the electron density of the B-ring, the conjugated system of tricin is expected to withdraw electrons.

The early onset of lignin degradation (within 1 week) found in this work further corroborates the presumption that the collective enzymatic machinery of *C. subvermispora* acts in concert with diffusible low-molecular-weight oxidants.[38−41] Such a proximal oxidant role has been ascribed to alk(en)-ylitaconic acids, sometimes referred to as "ceriporic acids", secondary metabolites produced abundantly by *C. subvermispora*.[39,42,43] These alkylitaconic acids can take part in ligninolytic MnP-mediated lipid peroxidation reactions, which were shown to proceed *threo*-diastereopreferentially.[44] As also discussed previously, the observed *threo*-preference in this work further corroborates the suggestion that delignification by *C. subvermispora* is initiated by single-electron transfer.[48,49] Enzymatic and chemical oxidations of lignin model compounds via an electron transfer mechanism have consistently shown a clear preference for the conversion of the *threo*-form, though it must be noted that this was only based on the disappearance of the initial substrate.[25,44,81,82] Cho et al. showed that SET oxidation of diastereomerically pure *β*-*O*-4′ dimers resulted in substantially more C_α-oxidized intact dimers for the *threo*-form, demonstrating that in fact the *erythro*-diastereomer was cleaved to a further extent.[83] Such "intact" oxidation products did not accumulate in our residual fungal-treated material, from which it is established that diastereoselective cleavage had indeed occurred.

The observations that *threo*-diastereomers of *β*-*O*-4′ aryl ethers were preferentially degraded and incorporation of *p*-coumarate (*p*-CA) at the *γ*-OH position increased resistance suggested that local steric hindrance and conformation might be major determinants for susceptibility against fungal degradation. Langer et al. showed that *threo*-forms of *β*-*O*-4′ aryl ethers existed in a more "extended" or "open" form and, consequently, might be more accessible to or promote interaction with the diffusible oxidants.[84] To the best of our knowledge, conformational studies on structural motifs exclusively occurring in grass lignin have not been performed. However, steric hindrance by *γ*-acylating *p*-coumaryl groups can be easily conceived. We postulate that this steric hindrance at the molecular level might affect diffusible oxidants as well as ligninolytic enzymes. Both need to be able to approach the structure in close enough proximity and/or in a certain configuration that allows for interaction and electron transfer.

CONCLUSIONS

This study has provided new insight into the delignification mechanisms of the biotechnologically relevant white-rot fungus *C. subvermispora*. We demonstrated that several structural motifs of wheat straw lignin differed in susceptibility to degradation. Our results imply that the electron density of the 4′-*O*-coupled ring and local steric hindrance determine the cleavage susceptibility of *β*-*O*-4′ aryl ethers. The susceptibility of these *β*-*O*-4′ aryl ether substructures is consistent with ligninolysis mechanisms that are initiated by single-electron transfer. We anticipate that the insights obtained will aid future efforts to improve the valorization of lignocellulosic biomass, first and foremost by presenting a structural rationale for selecting substrates that are more fit for purpose.

DOI: 10.1021/acssuschemeng.9b05780
ACS Sustainable Chem. Eng. 2019, 7, 20032−20042

■ ASSOCIATED CONTENT

Supporting Information

The Supporting Information is available free of charge at https://pubs.acs.org/doi/10.1021/acssuschemeng.9b05780.

Experimental details, carbohydrate content and composition, and additional data of py-GC-MS, SEC, and NMR analyses (PDF)

■ AUTHOR INFORMATION

Corresponding Author

*E-mail: mirjam.kabel@wur.nl. Tel: +31 317 483209.

ORCID

Antje Potthast: 0000-0003-1981-2271
Willem J. H. van Berkel: 0000-0002-6551-2782
Mirjam A. Kabel: 0000-0002-1544-1744

Notes

The authors declare no competing financial interest.

■ ACKNOWLEDGMENTS

Nazri Nayan, John W. Cone, Arend F. van Peer, and Anton S. M. Sonnenberg (Wageningen University & Research) are gratefully acknowledged for providing the *C. subvermispora*-treated wheat straw. We thank Christopher Lancefield (University of St Andrews) for discussion on the quantitativeness of HSQC NMR analyses. This article is based upon work from COST Action CA17128 "Establishment of a Pan-European Network on the Sustainable Valorisation of Lignin (LignoCOST)", supported by COST (European Cooperation in Science and Technology).

■ REFERENCES

(1) Ragauskas, A. J.; Williams, C. K.; Davison, B. H.; Britovsek, G.; Cairney, J.; Eckert, C. A.; Frederick, W. J., Jr.; Hallett, J. P.; Leak, D. J.; Liotta, C. L.; Mielenz, J. R.; Murphy, R.; Templer, R.; Tschaplinski, T. The path forward for biofuels and biomaterials. *Science* **2006**, *311*, 484−489.

(2) Behera, S.; Arora, R.; Nandhagopal, N.; Kumar, S. Importance of chemical pretreatment for bioconversion of lignocellulosic biomass. *Renewable Sustainable Energy Rev.* **2014**, *36*, 91−106.

(3) Isikgor, F. H.; Becer, C. R. Lignocellulosic biomass: a sustainable platform for the production of bio-based chemicals and polymers. *Polym. Chem.* **2015**, *6*, 4497−4559.

(4) Van Kuijk, S. J. A.; Sonnenberg, A. S. M.; Baars, J. J. P.; Hendriks, W. H.; Cone, J. W. Fungal treated lignocellulosic biomass as ruminant feed ingredient: a review. *Biotechnol. Adv.* **2015**, *33*, 191−202.

(5) Himmel, M. E.; Ding, S.-Y.; Johnson, D. K.; Adney, W. S.; Nimlos, M. R.; Brady, J. W.; Foust, T. D. Biomass recalcitrance: engineering plants and enzymes for biofuels production. *Science* **2007**, *315*, 804−807.

(6) Martínez, A. T.; Ruiz-Dueñas, F. J.; Martínez, M. J.; del Río, J. C.; Gutiérrez, A. Enzymatic delignification of plant cell wall: from nature to mill. *Curr. Opin. Biotechnol.* **2009**, *20*, 348−357.

(7) Hammel, K. E. Fungal Degradation of Lignin. In *Driven by Nature: Plant Litter Quality and Decomposition*; Cadish, G., Giller, K. E., Eds.; CAB-International: Wallingford, 1997; pp 33−47.

(8) Otjen, L.; Blanchette, R.; Effland, M.; Leatham, G. Assessment of 30 white rot basidiomycetes for selective lignin degradation. *Holzforschung* **1987**, *41*, 343−349.

(9) Tuyen, V.; Cone, J.; Baars, J.; Sonnenberg, A.; Hendriks, W. Fungal strain and incubation period affect chemical composition and nutrient availability of wheat straw for rumen fermentation. *Bioresour. Technol.* **2012**, *111*, 336−342.

(10) Tian, X.-f.; Fang, Z.; Guo, F. Impact and prospective of fungal pre-treatment of lignocellulosic biomass for enzymatic hydrolysis. *Biofuels, Bioprod. Biorefin.* **2012**, *6*, 335−350.

(11) Camarero, S.; Martínez, M. J.; Martínez, A. T. Understanding lignin biodegradation for the improved utilization of plant biomass in modern biorefineries. *Biofuels, Bioprod. Biorefin.* **2014**, *8*, 615−625.

(12) Sindhu, R.; Binod, P.; Pandey, A. Biological pretreatment of lignocellulosic biomass−An overview. *Bioresour. Technol.* **2016**, *199*, 76−82.

(13) van Erven, G.; Nayan, N.; Sonnenberg, A. S.; Hendriks, W. H.; Cone, J. W.; Kabel, M. A. Mechanistic insight in the selective delignification of wheat straw by three white-rot fungal species through quantitative ^{13}C-IS py-GC−MS and whole cell wall HSQC NMR. *Biotechnol Biofuels* **2018**, *11*, No. 262.

(14) van Kuijk, S. J. A.; Sonnenberg, A. S. M.; Baars, J. J. P.; Hendriks, W. H.; Del Río, J. C.; Rencoret, J.; Gutiérrez, A.; de Ruijter, N. C. A.; Cone, J. W. Chemical changes and increased degradability of wheat straw and oak wood chips treated with the white rot fungi *Ceriporiopsis subvermispora* and *Lentinula edodes*. *Biomass Bioenergy* **2017**, *105*, 381−391.

(15) Nayan, N.; Sonnenberg, A. S.; Hendriks, W. H.; Cone, J. W. Screening of white-rot fungi for bioprocessing of wheat straw into ruminant feed. *J. Appl. Microbiol.* **2018**, *125*, 468−479.

(16) Nayan, N.; van Erven, G.; Kabel, M. A.; Sonnenberg, A. S.; Hendriks, W. H.; Cone, J. W. Improving ruminal digestibility of various wheat straw types by white-rot fungi. *J. Sci. Food Agric.* **2019**, *99*, 957−965.

(17) Cianchetta, S.; Di Maggio, B.; Burzi, P. L.; Galletti, S. Evaluation of selected white-rot fungal isolates for improving the sugar yield from wheat straw. *Appl. Biochem. Biotechnol.* **2014**, *173*, 609−623.

(18) Wan, C.; Li, Y. Microbial pretreatment of corn stover with *Ceriporiopsis subvermispora* for enzymatic hydrolysis and ethanol production. *Bioresour. Technol.* **2010**, *101*, 6398−6403.

(19) Salvachúa, D.; Prieto, A.; López-Abelairas, M.; Lu-Chau, T.; Martínez, ÁT.; Martínez, M. J. Fungal pretreatment: an alternative in second-generation ethanol from wheat straw. *Bioresour. Technol.* **2011**, *102*, 7500−7506.

(20) Akhtar, M.; Attridge, M. C.; Myers, G. C.; Blanchette, R. A. Biomechanical pulping of loblolly pine chips with selected white-rot fungi. *Holzforschung* **1993**, *47*, 36−40.

(21) Ferraz, A.; Guerra, A.; Mendonça, R.; Masarin, F.; Vicentim, M. P.; Aguiar, A.; Pavan, P. C. Technological advances and mechanistic basis for fungal biopulping. *Enzyme Microb. Technol.* **2008**, *43*, 178−185.

(22) Wan, C.; Li, Y. Fungal pretreatment of lignocellulosic biomass. *Biotechnol. Adv.* **2012**, *30*, 1447−1457.

(23) Fernández-Fueyo, E.; Ruiz-Dueñas, F. J.; Ferreira, P.; Floudas, D.; Hibbett, D. S.; Canessa, P.; Larrondo, L. F.; James, T. Y.; Seelenfreund, D.; Lobos, S.; Polanco, R.; Tello, M.; Honda, Y.; Watanabe, T.; Watanabe, T.; Ryu, J. S.; Kubicek, C. P.; Schmoll, M.; Gaskell, J.; Hammel, K. E.; St. John, F. J.; Vanden Wymelenberg, A.; Sabat, G.; Splinter Bondurant, S.; Khajamohiddin, S.; Jagit, Y. S.; Doppapaneni, H.; Subramanian, V.; José, L. L.; Oguiza, J. A.; Perez, G.; Pisabarro, A. G.; Ramirez, L.; Santoyo, F.; Master, E.; Coutinho, P. M.; Henrissat, B.; Lombard, V.; Magnuson, J. K.; Kües, U.; Hori, C.; Igarashi, K.; Samejima, M.; Held, B. W.; Barry, K. W.; Labutti, K. M.; Lapidus, A.; Lindquist, E. A.; Lucas, S. M.; Riley, R.; Salamov, A. A.; Hoffmeister, D.; Schwenk, D.; Hadar, Y.; Yarden, O.; de Vries, R. P.; Wiebenga, A.; Stenlid, J.; Eastwood, D.; Grigoriev, I. V.; Berka, R. M.; Blanchette, R. A.; Kersten, P.; Martínez, A. T.; Vicuna, R.; Cullen, D. Comparative genomics of *Ceriporiopsis subvermispora* and *Phanerochaete chrysosporium* provide insight into selective ligninolysis. *Proc. Natl. Acad. Sci. U.S.A.* **2012**, *109*, 5458−5463.

(24) Hori, C.; Gaskell, J.; Igarashi, K.; Kersten, P.; Mozuch, M.; Samejima, M.; Cullen, D. Temporal alterations in secretome of selective ligninolytic fungi *Ceriporiopsis subvermispora* during growth on aspen wood reveal its strategy of degrading lignocellulose. *Appl. Environ. Microbiol.* **2014**, *80*, 2062−2070.

DOI: 10.1021/acssuschemeng.9b05780
ACS Sustainable Chem. Eng. 2019, 7, 20032−20042

(25) Fernández-Fueyo, E.; Ruiz-Dueñas, F. J.; Miki, Y.; Martínez, M. J.; Hammel, K. E.; Martínez, A. T. Lignin-degrading peroxidases from genome of selective ligninolytic fungus *Ceriporiopsis subvermispora*. *J. Biol. Chem.* **2012**, *287*, 16903−16916.
(26) Srebotnik, E.; Jensen, K.; Kawai, S.; Hammel, K. E. Evidence that *Ceriporiopsis subvermispora* degrades nonphenolic lignin structures by a one-electron-oxidation mechanism. *Appl. Environ. Microbiol.* **1997**, *63*, 4435−4440.
(27) Jensen, K. A.; Bao, W.; Kawai, S.; Srebotnik, E.; Hammel, K. E. Manganese-dependent cleavage of nonphenolic lignin structures by *Ceriporiopsis subvermispora* in the absence of lignin peroxidase. *Appl. Environ. Microbiol.* **1996**, *62*, 3679−3686.
(28) Daina, S.; Orlandi, M.; Bestetti, G.; Wiik, C.; Elegir, G. Degradation of β-5 lignin model dimers by *Ceriporiopsis subvermispora*. *Enzyme Microb. Technol.* **2002**, *30*, 499−505.
(29) Vanholme, R.; Demedts, B.; Morreel, K.; Ralph, J.; Boerjan, W. Lignin biosynthesis and structure. *Plant Physiol.* **2010**, *153*, 895−905.
(30) Del Río, J. C.; Rencoret, J.; Prinsen, P.; Martínez, A. T.; Ralph, J.; Gutiérrez, A. Structural characterization of wheat straw lignin as revealed by analytical pyrolysis, 2D-NMR, and reductive cleavage methods. *J. Agric. Food Chem.* **2012**, *60*, 5922−5935.
(31) Akiyama, T.; Goto, H.; Nawawi, D. S.; Syafii, W.; Matsumoto, Y.; Meshitsuka, G. Erythro/threo ratio of β-O-4 structures as an important structural characteristic of lignin. Part 4: Variation in the erythro/threo ratio in softwood and hardwood lignins and its relation to syringyl/guaiacyl ratio. *Holzforschung* **2005**, *59*, 276−281.
(32) Ralph, J.; Brunow, G.; Harris, P. J.; Dixon, R. A.; Schatz, P. F.; Boerjan, W. Lignification: Are Lignins Biosynthesized via Simple Combinatorial Chemistry or via Proteinaceous Control and Template Replication?. In *Recent Advances in Polyphenol Research*; Lattanzio, V., Daayf, F., Eds.; Wiley-Blackwell: Oxord, 2009; Vol. *1*, pp 36−66.
(33) Crestini, C.; Argyropoulos, D. S. Structural analysis of wheat straw lignin by quantitative 31P and 2D NMR spectroscopy. The occurrence of ester bonds and α-O-4 substructures. *J. Agric. Food Chem.* **1997**, *45*, 1212−1219.
(34) Ralph, J.; Bunzel, M.; Marita, J. M.; Hatfield, R. D.; Lu, F.; Kim, H.; Schatz, P. F.; Grabber, J. H.; Steinhart, H. Peroxidase-dependent cross-linking reactions of p-hydroxycinnamates in plant cell walls. *Phytochem. Rev.* **2004**, *3*, 79−96.
(35) Ralph, J. Hydroxycinnamates in lignification. *Phytochem. Rev.* **2010**, *9*, 65−83.
(36) Lan, W.; Lu, F.; Regner, M.; Zhu, Y.; Rencoret, J.; Ralph, S. A.; Zakai, U. I.; Morreel, K.; Boerjan, W.; Ralph, J. Tricin, a flavonoid monomer in monocot lignification. *Plant Physiol.* **2015**, *167*, 1284−1295.
(37) Lan, W.; Rencoret, J.; Lu, F.; Karlen, S. D.; Smith, B. G.; Harris, P. J.; Río, J. C.; Ralph, J. Tricin-lignins: occurrence and quantitation of tricin in relation to phylogeny. *Plant J.* **2016**, *88*, 1046−1057.
(38) Blanchette, R. A.; Krueger, E. W.; Haight, J. E.; Akhtar, M.; Akin, D. E. Cell wall alterations in loblolly pine wood decayed by the white-rot fungus, *Ceriporiopsis subvermispora*. *J. Biotechnol.* **1997**, *53*, 203−213.
(39) Enoki, M.; Watanabe, T.; Nakagame, S.; Koller, K.; Messner, K.; Honda, Y.; Kuwahara, M. Extracellular lipid peroxidation of selective white-rot fungus, *Ceriporiopsis subvermispora*. *FEMS Microbiol. Lett.* **1999**, *180*, 205−211.
(40) Kirk, T. K.; Cullen, D. Enzymology and Molecular Genetics of Wood Degradation by White-Rot Fungi. In *Environmentally Friendly Technologies for the Pulp and Paper Industry*; Young, R., Akhtar, M., Eds.; Wiley: New York, 1998; pp 273−307.
(41) Fackler, K.; Gradinger, C.; Hinterstoisser, B.; Messner, K.; Schwanninger, M. Lignin degradation by white rot fungi on spruce wood shavings during short-time solid-state fermentations monitored by near infrared spectroscopy. *Enzyme Microb. Technol.* **2006**, *39*, 1476−1483.
(42) Gutiérrez, A.; del Río, J. C.; Martínez-Íñigo, M. J.; Martínez, M. J.; Martínez, Á. T. Production of new unsaturated lipids during wood decay by ligninolytic basidiomycetes. *Appl. Environ. Microbiol.* **2002**, *68*, 1344−1350.
(43) Amirta, R.; Fujimori, K.; Shirai, N.; Honda, Y.; Watanabe, T. Ceriporic acid C, a hexadecenylitaconate produced by a lignin-degrading fungus, *Ceriporiopsis subvermispora*. *Chem. Phys. Lipids* **2003**, *126*, 121−131.
(44) Nishimura, H.; Sasaki, M.; Seike, H.; Nakamura, M.; Watanabe, T. Alkadienyl and alkenyl itaconic acids (ceriporic acids G and H) from the selective white-rot fungus *Ceriporiopsis subvermispora*: a new class of metabolites initiating ligninolytic lipid peroxidation. *Org. Biomol. Chem.* **2012**, *10*, 6432−6442.
(45) Guerra, A.; Mendonça, R.; Ferraz, A.; Lu, F.; Ralph, J. Structural characterization of lignin during *Pinus taeda* wood treatment with *Ceriporiopsis subvermispora*. *Appl. Environ. Microbiol.* **2004**, *70*, 4073−4078.
(46) Choi, J.; Choi, D.; Ahn, S.; Lee, S.; Kim, M.; Meier, D.; Faix, O.; Scott, G. M. Characterization of trembling aspen wood (*Populus tremuloides* L.) degraded with the white rot fungus *Ceriporiopsis subvermispora* and MWLs isolated thereof. *Holz Roh- Werkst.* **2006**, *64*, 415−422.
(47) Amirta, R.; Tanabe, T.; Watanabe, T.; Honda, Y.; Kuwahara, M.; Watanabe, T. Methane fermentation of Japanese cedar wood pretreated with a white rot fungus, *Ceriporiopsis subvermispora*. *J. Biotechnol.* **2006**, *123*, 71−77.
(48) Yelle, D. J.; Kapich, A. N.; Houtman, C. J.; Lu, F.; Timokhin, V. I.; Fort, R. C.; Ralph, J.; Hammel, K. E. A highly diastereoselective oxidant contributes to ligninolysis by the white rot basidiomycete *Ceriporiopsis subvermispora*. *Appl. Environ. Microbiol.* **2014**, *80*, 7536−7544.
(49) van Erven, G.; Hilgers, R.; de Waard, P.; Gladbeek, E.-J.; van Berkel, W. J. H.; Kabel, M. A. Elucidation of in situ ligninolysis mechanisms of the selective white-rot fungus *Ceriporiopsis subvermispora*. *ACS Sustainable Chem. Eng.* **2019**, *7*, 16757−16764.
(50) Nayan, N.; Sonnenberg, A. S. M.; Hendriks, W. H.; Cone, J. W. Differences between two strains of *Ceriporiopsis subvermispora* on improving the nutritive value of wheat straw for ruminants. *J. Appl. Microbiol.* **2017**, *123*, 352−361.
(51) Björkman, A. Studies on finely divided wood. Part 1. Extraction of lignin with neutral solvents. *Sven. Papperstidn.* **1956**, *59*, 477−485.
(52) Chang, H.-m.; Cowling, E. B.; Brown, W. Comparative studies on cellulolytic enzyme lignin and milled wood lignin of sweetgum and spruce. *Holzforschung* **1975**, *29*, 153−159.
(53) van Erven, G.; de Visser, R.; Merkx, D. W.; Strolenberg, W.; De Gijsel, P.; Gruppen, H.; Kabel, M. A. Quantification of lignin and its structural features in plant biomass using ^{13}C lignin as internal standard for pyrolysis-GC-SIM-MS. *Anal. Chem.* **2017**, *89*, 10907−10916.
(54) Kim, H.; Ralph, J.; Akiyama, T. Solution-state 2D NMR of ball-milled plant cell wall gels in DMSO-d_6. *BioEnergy Res.* **2008**, *1*, 56−66.
(55) Mansfield, S. D.; Kim, H.; Lu, F.; Ralph, J. Whole plant cell wall characterization using solution-state 2D NMR. *Nat. Protoc.* **2012**, *7*, 1579−1589.
(56) Ralph, S. A.; Ralph, J.; Landucci, L. NMR Database of Lignin and Cell Wall Model Compounds, 2009. Available at URL www.glbrc.org/databases_and_software/nmrdatabase/.
(57) Rencoret, J.; Gutiérrez, A.; Nieto, L.; Jiménez-Barbero, J.; Faulds, C. B.; Kim, H.; Ralph, J.; Martínez, Á. T.; José, C. Lignin composition and structure in young versus adult *Eucalyptus globulus* plants. *Plant Physiol.* **2011**, *155*, 667−682.
(58) Rencoret, J.; Pereira, A.; del Río, J. C.; Martínez, Á. T.; Gutiérrez, A. Delignification and saccharification enhancement of sugarcane byproducts by a laccase-based pretreatment. *ACS Sustainable Chem. Eng.* **2017**, *5*, 7145−7154.
(59) del Río, J. C.; Lino, A. G.; Colodette, J. L.; Lima, C. F.; Gutiérrez, A.; Martínez, Á. T.; Lu, F.; Ralph, J.; Rencoret, J. Differences in the chemical structure of the lignins from sugarcane bagasse and straw. *Biomass Bioenergy* **2015**, *81*, 322−338.
(60) Kim, H.; Padmakshan, D.; Li, Y.; Rencoret, J.; Hatfield, R. D.; Ralph, J. Characterization and elimination of undesirable protein residues in plant cell wall materials for enhancing lignin analysis by

DOI: 10.1021/acssuschemeng.9b05780
ACS Sustainable Chem. Eng. 2019, 7, 20032−20042

solution-state nuclear magnetic resonance spectroscopy. *Biomacromolecules* **2017**, *18*, 4184−4195.
(61) Lan, W.; Yue, F.; Rencoret, J.; del Río, J.; Boerjan, W.; Lu, F.; Ralph, J. Elucidating tricin-lignin structures: assigning correlations in HSQC spectra of monocot lignins. *Polymers* **2018**, *10*, No. 916.
(62) Gosselink, R. J. A.; van Dam, J. E. G.; de Jong, E.; Scott, E. L.; Sanders, J. P. M.; Li, J.; Gellerstedt, G. Fractionation, analysis, and PCA modeling of properties of four technical lignins for prediction of their application potential in binders. *Holzforschung* **2010**, *64*, 193−200.
(63) Granata, A.; Argyropoulos, D. S. 2-Chloro-4,4,5,5-tetramethyl-1,3,2-dioxaphospholane, a reagent for the accurate determination of the uncondensed and condensed phenolic moieties in lignins. *J. Agric. Food Chem.* **1995**, *43*, 1538−1544.
(64) Constant, S.; Wienk, H. L. J.; Frissen, A. E.; de Peinder, P.; Boelens, R.; Van Es, D. S.; Grisel, R. J. H.; Weckhuysen, B. M.; Huijgen, W. J. J.; Gosselink, R. J. A.; Bruijnincx, P. C. A. New insights into the structure and composition of technical lignins: a comparative characterisation study. *Green Chem.* **2016**, *18*, 2651−2665.
(65) Zinovyev, G.; Sulaeva, I.; Podzimek, S.; Rössner, D.; Kilpeläinen, I.; Sumerskii, I.; Rosenau, T.; Potthast, A. Getting closer to absolute molar masses of technical lignins. *ChemSusChem* **2018**, *11*, 3259−3268.
(66) Sulaeva, I.; Zinovyev, G.; Plankeele, J. M.; Sumerskii, I.; Rosenau, T.; Potthast, A. Fast track to molar-mass distributions of technical lignins. *ChemSusChem* **2017**, *10*, 629−635.
(67) Englyst, H. N.; Cummings, J. H. Simplified method for the measurement of total non-starch polysaccharides by gas-liquid chromatography of constituent sugars as alditol acetates. *Analyst* **1984**, *109*, 937−942.
(68) Jiang, B.; Cao, T.; Gu, F.; Wu, W.; Jin, Y. Comparison of the structural characteristics of cellulolytic enzyme lignin preparations isolated from wheat straw stem and leaf. *ACS Sustainable Chem. Eng.* **2017**, *5*, 342−349.
(69) Zikeli, F.; Ters, T.; Fackler, K.; Srebotnik, E.; Li, J. Successive and quantitative fractionation and extensive structural characterization of lignin from wheat straw. *Ind. Crops Prod.* **2014**, *61*, 249−257.
(70) Del Río, J.; Martin, F.; Gonzalez-Vila, F. Thermally assisted hydrolysis and alkylation as a novel pyrolytic approach for the structural characterization of natural biopolymers and geomacromolecules. *TrAC, Trends Anal. Chem.* **1996**, *15*, 70−79.
(71) Del Río, J. C.; Gutiérrez, A.; Rodríguez, I. M.; Ibarra, D.; Martínez, A. T. Composition of non-woody plant lignins and cinnamic acids by Py-GC/MS, Py/TMAH and FT-IR. *J. Anal. Appl. Pyrolysis* **2007**, *79*, 39−46.
(72) Zeng, J.; Helms, G. L.; Gao, X.; Chen, S. Quantification of wheat straw lignin structure by comprehensive NMR analysis. *J. Agric. Food Chem.* **2013**, *61*, 10848−10857.
(73) Lancefield, C. S.; Wienk, H. L.; Boelens, R.; Weckhuysen, B. M.; Bruijnincx, P. C. Identification of a diagnostic structural motif reveals a new reaction intermediate and condensation pathway in kraft lignin formation. *Chem. Sci.* **2018**, *9*, 6348−6360.
(74) Kupče, E.; Freeman, R. Compensated adiabatic inversion pulses: broadband INEPT and HSQC. *J. Magn. Reson.* **2007**, *187*, 258−265.
(75) Xia, Z.; Akim, L. G.; Argyropoulos, D. S. Quantitative 13C NMR analysis of lignins with internal standards. *J. Agric. Food Chem.* **2001**, *49*, 3573−3578.
(76) Martínez, A. T.; Rencoret, J.; Nieto, L.; Jiménez-Barbero, J.; Gutiérrez, A.; del Río, J. C. Selective lignin and polysaccharide removal in natural fungal decay of wood as evidenced by in situ structural analyses. *Environ. Microbiol.* **2011**, *13*, 96−107.
(77) Hammel, K. E.; Cullen, D. Role of fungal peroxidases in biological ligninolysis. *Curr. Opin. Plant Biol.* **2008**, *11*, 349−355.
(78) Wong, D. W. Structure and action mechanism of ligninolytic enzymes. *Appl. Biochem. Biotechnol.* **2009**, *157*, 174−209.
(79) Martínez, A.; Camarero, S.; Gutiérrez, A.; Bocchini, P.; Galletti, G. Studies on wheat lignin degradation by *Pleurotus* species using analytical pyrolysis. *J. Anal. Appl. Pyrolysis* **2001**, *58*, 401−411.
(80) Lan, W.; Morreel, K.; Lu, F.; Rencoret, J.; del Río, J. C.; Voorend, W.; Vermerris, W.; Boerjan, W.; Ralph, J. Maize tricin-oligolignol metabolites and their implications for monocot lignification. *Plant Physiol.* **2016**, *171*, 810−820.
(81) Bohlin, C.; Andersson, P.-O.; Lundquist, K.; Jönsson, L. J. Differences in stereo-preference in the oxidative degradation of diastereomers of the lignin model compound 1-(3, 4-dimethoxyphenyl)-2-(2-methoxyphenoxy)-1, 3-propanediol with enzymic and non-enzymic oxidants. *J. Mol. Catal. B: Enzym.* **2007**, *45*, 21−26.
(82) Bohlin, C.; Lundquist, K.; Jönsson, L. J. Diastereomer selectivity in the degradation of a lignin model compound of the arylglycerol *β*-aryl ether type by white-rot fungi. *Enzyme Microb. Technol.* **2008**, *43*, 199−204.
(83) Cho, D. W.; Parthasarathi, R.; Pimentel, A. S.; Maestas, G. D.; Park, H. J.; Yoon, U. C.; Dunaway-Mariano, D.; Gnanakaran, S.; Langan, P.; Mariano, P. S. Nature and kinetic analysis of carbon−carbon bond fragmentation reactions of cation radicals derived from set-oxidation of lignin model compounds. *J. Org. Chem.* **2010**, *75*, 6549−6562.
(84) Langer, V.; Lundquist, K.; Parkås, J. The stereochemistry and conformation of lignin as judged by X-ray crystallographic investigations of lignin model compounds: arylglycerol *β*-guaiacyl ethers. *BioResources* **2007**, *2*, 590−597.

DOI: 10.1021/acssuschemeng.9b05780
ACS Sustainable Chem. Eng. 2019, 7, 20032−20042